THE ASTROPHYSICAL JOURNAL, 539:424–434, 2000 August 10

THE DISK OF β PICTORIS IN THE LIGHT OF POLARIMETRIC DATA

NATALIA A. KRIVOVA,[1] ALEXANDER V. KRIVOV,[1] AND INGRID MANN[2]
Max-Planck-Institut für Aeronomie, D-37191, Katlenburg-Lindau, Germany; natalie@linmpi.mpg.de, krivov@linmpi.mpg.de, mann@linmpi.mpg.de
Received 1999 December 2; accepted 2000 March 13

ABSTRACT

We model the linear polarization of the radiation of β Pic scattered by dust particles in the circumstellar disk. The observed spatial distribution and the wavelength dependence of the polarization together with the colors of the β Pic disk require that particles in a wide size range be present in the disk, with the grains smaller than a few microns in size being somewhat depleted but still of importance for the polarization and colors. The inferred size distribution is consistent with the production and loss mechanisms: the sources—presumably collisions and evaporation of large bodies—continuously produce dust with a power-law size distribution with the exponent ~ 3.5 over a broad range of sizes, but the particles smaller than a few microns are blown away by the radiation pressure, which shortens the time they spend in the disk and decreases their number densities. Compact (or slightly porous) silicates are found to give better agreement with the observations, although other materials are still not ruled out and a high fluffiness of the large particles is possible. The observed asymmetry in the polarization of two wings can be explained if more small grains (by 20%–30%) are present on the northeast side of the disk. We show that such an asymmetry in the size distributions in two wings might be caused by an influence of the interstellar medium; a required amount of small grains could be produced by destructive collisions of interstellar grains with the circumstellar dust particles.

Subject headings: circumstellar matter — polarization — stars: individual (β Pictoris)

1. INTRODUCTION

Polarization measurements are an important tool to study properties of dust in different environments, such as the zodiacal cloud and cometary dust, dust in the interstellar medium, and dust around other stars including disks and shells around young and main-sequence stars. We concentrate here on the circumstellar disk of β Pic—the most explored among Vega-type objects, which has been attracting considerable interest from researchers since its discovery by Aumann et al. (1984).

The observed linear polarization of the disk in the R band is well fitted with the empirical scattering and polarization functions of the zodiacal cloud (Artymowicz 1997; Krivova, Mann, & Krivov 1999), which is probably not surprising. The dust in the circumstellar disk of β Pic does really resemble (except for the higher albedo) dust in the solar system (see Artymowicz 1997 and references therein). It is believed that, similarly to the dust in our solar system, the dust material is supplied by larger parent bodies. Next, the dust around β Pic has a wide size distribution extending to macroscopic bodies, with the largest area contribution coming from particles of about 1–10 μm in size. Finally, the profile of the 10 μm silicate emission feature is similar to that observed for comet Halley (Telesco & Knacke 1991; Knacke et al. 1993; Aitken et al. 1993).

Despite this similarity, however, and in contrast to the fairly well established geometry of the disk (see, e.g., Artymowicz 1994 and Artymowicz 1997 for details), the properties of the dust around β Pic are not well known. The results obtained from consideration of different observational data diverge considerably (cf. the discussion in Li & Greenberg 1998). Gray colors of the disk (Smith & Terrile 1987; Paresce & Burrows 1987; Lecavelier des Etangs et al. 1993) tell us that the particles are typically larger than a few microns. To explain both the visible and IR observations, particles of about 1–20 μm in size are required (Artymowicz, Paresce, & Burrows 1990). The grains should be larger than 5–10 μm to fit the far-IR and millimeter data available (Chini et al. 1991; Zuckerman & Becklin 1993). The observed profile of the 10 μm silicate feature indicates the particles to be smaller than 10 μm, the most probable sizes being about 2–3 μm (Telesco & Knacke 1991; Aitken et al. 1993). Grains of 1 μm size and even smaller were found to be most suitable from consideration of *IRAS* and ground-based IR data (Backman, Witteborn, & Gillett 1992). The presence of submicron grains is also evidenced by the flux densities at 10 μm and 20 μm (Telesco et al. 1988). However, particles smaller than about 2 μm should be quickly swept out by the stellar radiation pressure (Artymowicz 1988).

In this paper the available polarization data of the system are used to gain better insight into the properties of dust. Attempts to understand the dust properties from study of the polarization had already been undertaken by Scarrott, Draper, & Gledhill (1992) and by Voshchinnikov & Krügel (1999). However, the wavelength dependence of the polarization was not yet available to Scarrott et al. (1992), and it is this dependence that provides the main information about the dust properties. Voshchinnikov & Krügel (1999) have clearly shown that, independent of the dust grain composition and structure, polarization diagrams, and hence the observed polarization, are predominantly determined by the particle sizes, which is to say that polarization carries information about the sizes. Despite this fact in both papers, the analysis was confined to power-law size distributions of dust grains, for which we propose and justify a better substitution. Besides, the authors fitted observations in both wings of the disk together, although the polarization in the two wings is significantly different (Wolstencroft, Scarrott, & Gledhill 1995). In contrast, we fit the data for each wing separately and show the difference between the dust properties there.

[1] On leave from Astronomical Institute, St. Petersburg University, 198904 St. Petersburg, Russia.
[2] Also at California Institute of Technology, Pasadena, CA.

The observational data are described in § 2. Although in the paper we pay attention mainly to the spatially resolved data (§ 2.2), we first discuss briefly the available integral polarization observations (§ 2.1), taking, therewith, a quick look at the data for a few other Vega-type candidates. In § 3 we describe our model: the main equations (§ 3.1), geometry of the shell (§ 3.2), and the dust grain model (§ 3.3). First, we modified a commonly used power-law distribution, and then the distribution that could be settled in the disk as a result of the dust dynamical evolution. The polarization calculated for the southwest wing with these two models is discussed in § 4. Asymmetry of the wings is addressed in § 5. In addition, we consider interactions of the circumstellar grains with interstellar dust as a possible source of the observed asymmetry (Lissauer & Griffith 1989; Artymowicz & Clampin 1997). Section 6 contains our conclusions.

2. OBSERVATIONAL DATA

2.1. *Integral Polarization*

The total linear polarization of β Pic measured by Tinbergen (1982) in a broad band between 0.4 and 0.7 μm is $P = 0.020\% \pm 0.008\%$ (polarization degree), $\theta = 94^\circ \pm 11^\circ$ (position angle of polarization). Being a close star ($d = 19.3$ pc; Crifo et al. 1997), β Pic undergoes little interstellar extinction and polarization (Tinbergen 1982; Leroy 1993, 1999), which, however, needs to be estimated.

We selected all the stars with measured polarization in the visual from the same part of the sky as β Pic at distances less than 40 pc (Mathewson & Ford 1970; Schröder 1976; Krautter 1980; Tinbergen 1982; Korhonen & Reiz 1986; Leroy 1993). Leroy (1993), unfortunately, does not provide the polarization angles for his observations. The low density of dust in the Local Bubble (Tinbergen 1982; Leroy 1993, 1999) makes the analysis of the polarimetric data a bit troublesome, since the typical values of the polarization are very low and often close to the detection limit. At the final sample we dropped the data of Mathewson & Ford (1970) as having errors too large for our purpose. Variable stars and close binaries were excluded as well. When analyzing the distribution of the observed polarization angles, we also rejected the stars, for which the measurement error was larger than the value of the polarization, since in this case the angles were very uncertain. Finally, a few stars—the Vega-type candidates discussed below—were eliminated from the sample.

The polarization of the sample stars as a function of their distances from the Sun is depicted in Figure 1*a*. Whenever possible, we used the distances obtained from *Hipparcos* data (Turon et al. 1993; Hünsch, Schmitt, & Voges 1998; Hünsch et al. 1999; Schröder, Hünsch, & Schmitt 1998). Also shown is the field of the observed polarization angles. The fair homogeneity of the Local Bubble (Tinbergen 1982; Leroy 1993, 1999) suggests that the interstellar polarization can be approximately described by a linear function of distance. Therefore we draw a linear fit through the data and compare the polarization of individual stars with this linear fit. The polarization of β Pic is about twice as high as the average polarization of other stars at similar distances, which might indicate that the polarization stems from a different effect. Another indication of a different origin of its polarization is the polarization angle differing from the dominant direction.

In contrast, α Pic, being one of the closest stars to β Pic and having a similar spectral type, shows a polarization very typical for the area: $P = 0.012\% \pm 0.008\%$, $\theta = 47^\circ \pm 17^\circ$. As a comparison star it was observed by Gledhill, Scarrott, & Wolstencroft (1991) in their imaging polarimetry of β Pic. Unlike β Pic, it showed no polarization pattern or images of a disk. Thus we can use the data

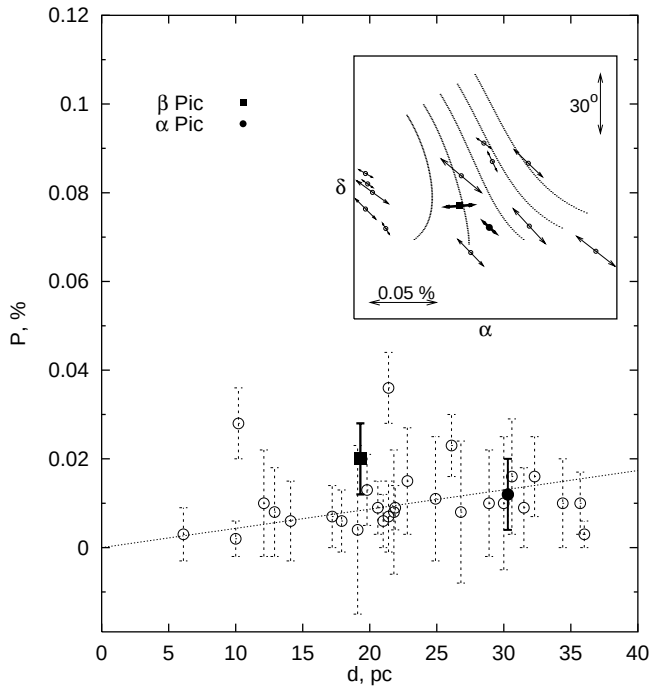

FIG. 1*a*

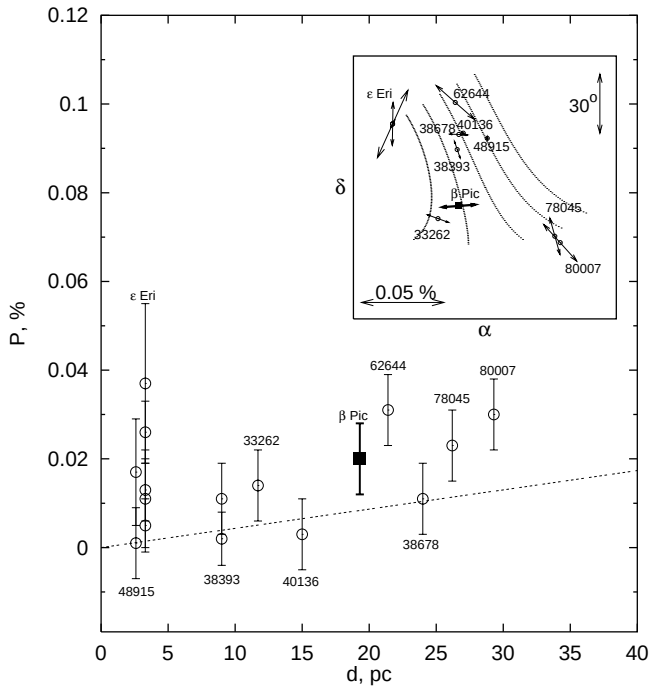

FIG. 1*b*

FIG. 1.—(*a*) Polarization degree of the field stars in the vicinity of β Pic (see text for the selection criteria) as a function of distance. The dotted line is a linear fit through these data. The inset at the upper right corner shows the polarization vectors. Dotted lines in the inset are lines of constant Galactic latitude. (*b*) Same as (*a*), but for possible Vega-type candidates.

for α Pic to eliminate the interstellar contribution. The obtained intrinsic polarization of the light of β Pic is then $P = 0.024\% \pm 0.011\%$, $\theta = 109^\circ \pm 13^\circ$. Since the position angle of the disk of β Pic is about 30°, this implies that the polarization vector is, within the limits of observational errors, perpendicular to the disk. This could really be expected for the polarization arising in an optically thin dust disk.

We calculated the integral polarization of the disk around β Pic (see § 3) with the zodiacal cloud empirical scattering and polarization functions. For an optically thin spherical dust envelope, the intensity and hence the polarization of scattered light are proportional to the product $\tau\Lambda$ of the optical depth and albedo (Sobolev 1985). Our results show that the law $P \propto \tau\Lambda$, where τ is the edge-on optical depth, holds true for an optically thin dust disk. The polarization depends also on a viewing angle of the disk (Krivova et al. 1999), but the difference within the range 0°–10° supposed for β Pic is small. The edge-on optical depth and the albedo of the dust inferred from the modeling of different observations of β Pic are about 0.03–0.07 (Artymowicz et al. 1990) and 0.5 ± 0.2 (Artymowicz 1997), respectively. For these ranges the calculated integral polarization is 0.01%–0.04%. In particular, $P \approx 0.020\%$–0.025% when $\tau = 0.05$ and $\Lambda = 0.5$. So the values of the optical depth and albedo for the disk of β Pic obtained earlier from consideration of other data are in agreement with the observed level of its polarization.

When collecting data about the stars in the direction of β Pic we found, as noted above, that a few stars from our sample were considered as possible candidates to Vega-type stars. They are HD 33262, HD 38393, HD 38678, HD 40136, HD 48915, HD 62644, HD 78045, and HD 80007 (Backman & Gillett 1987; Aumann 1988; Aumann & Probst 1991; Cheng et al. 1992; Backman & Paresce 1993; Fajardo-Acosta, Telesco, & Knacke 1998; Mannings & Barlow 1998). The polarization as a function of the distance and the polarization angles for these stars are presented in Figure 1*b*. In addition, the data for ϵ Eri, another Vega-like source located fairly close to the considered area, are included (Serkowski 1968; Schröder 1976; Tinbergen 1982; Korhonen & Reiz 1986; Leroy & Le Borgne 1989; Leroy 1993). A difference with Figure 1*a* is noticeable and makes it clear why we eliminated these stars. Obviously, the integral intrinsic polarization of Vega-type candidates is too small (which would really be expected for the observed levels of the IR excesses), the measurement accuracies being too low to be considered as evidence of the dust disk around a particular star. Nevertheless, the observed polarization of the candidates could, at least partly, be of circumstellar origin, which is evidenced by the polarization level typically higher than the average, as well as by the dissimilar polarization angles.

2.2. *Spatially Resolved Data*

An imaging photometry of β Pic was performed in the R band by Gledhill et al. (1991) between 15″ and 30″ and in the B, V, R, and I bands by Wolstencroft et al. (1995) between 8″ and 15″. The polarization of the disk as a function of offset distance from the star ranges from 10% to 25% in different bands, with an average of 15%–17%.

The polarization in the northeast wing is almost constant and independent of the wavelength. The polarization in the southwest wing grows with the wavelength and changes distinctly with the offset. Such behavior would be expected if the particles in the northeast wing were typically smaller than on the southwest side (see, e.g., Martin 1978).

It should be added that the disk was found to have the same color as the star (Paresce & Burrows 1987; Smith & Terrile 1987; Lecavelier des Etangs et al. 1993). The relative colors $Q_i(r) = (N_i^d/N_I^d)/(N_i^*/N_I^*)$, where N_i^d and N_I^d represent the (relative) fluxes from the disk in the i and I bands, respectively, while N_i^* and N_I^* stand for the corresponding fluxes from unobstructed β Pic, were found by Paresce & Burrows (1987) to be $Q_B = 0.84 \pm 0.28$, $Q_V = 1.01 \pm 0.22$, and $Q_R = 1.21 \pm 0.24$. Within 12″ from the star the colors are independent of the offset distance, with a probable exception in the region close to the star ($\lesssim 2\farcs5$), where the disk color in the blue (B) drops down (Lecavelier des Etangs et al. 1993).

3. MODEL

3.1. *Main Equations*

The disk of β Pic is optically thin; the midplane optical depth in the visual is less than 0.1 (e.g., Artymowicz et al. 1990; Artymowicz 1997). Therefore, the single-scattering approximation is well founded.

Consider light scattering by a single dust grain. Define the Cartesian coordinate system $X_1Y_1Z_1$ as follows: the X_1-axis is perpendicular to the scattering plane star-grain-observer; Y_1 lies in the scattering plane; and Z_1 points from the grain to the observer. The irradiances of the scattered light for incident light polarized in directions perpendicular and parallel to the scattering plane (i.e., along X_1 and Y_1), $i_\perp$ and $i_\parallel$, respectively, are written as

$$i_\perp = \tfrac{1}{2} i(\Theta)[1 + p_f(\Theta)] ,$$
$$i_\parallel = \tfrac{1}{2} i(\Theta)[1 - p_f(\Theta)] ,$$

where Θ is the scattering angle, $p_f(\Theta)$ is the polarization function, and $i(\Theta)$ is the scattering function.

Introduce now the coordinate system centered on the star, XYZ: the X-axis is directed from the star toward the observer, Y lies in the symmetry plane of the disk and is perpendicular to X, Z is perpendicular to the line of sight and completes the right triad. Denote by δ the angle between the X-Y plane and the scattering plane Y_1-Z_1. The Stokes parameters $\boldsymbol{S}_g \equiv \{I_g, U_g, Q_g\}$ in XYZ,

$$I_g = i_\perp + i_\parallel ,$$
$$Q_g = (i_\perp - i_\parallel) \cos(2\delta) ,$$
$$U_g = (i_\perp - i_\parallel) \sin(2\delta) ,$$

describe the polarization of light scattered by one grain. The Stokes parameters $\boldsymbol{S} \equiv \{I, U, Q\}$ that characterize the observed polarization of light coming from a given area $\Delta y \Delta z$ of the disk centered on (y, z) are determined by

$$\boldsymbol{S}(y, z, \Delta y, \Delta z) = \Delta y \Delta z \int_{-x_{\max}}^{x_{\max}} \boldsymbol{S}_g \, n(x, y, z) dx , \qquad (1)$$

where $n(x, y, z)$ is the number density of dust and the integral is taken along the X-axis within the disk. The observed polarization degree of light coming from the same area then reads

$$P(y, z, \Delta y, \Delta z) = (Q^2 + U^2)^{1/2}/I . \qquad (2)$$

By integrating the Stokes parameters over the height of the disk (along the Z-axis), which is confined to a half–opening angle $\sim 7^\circ$ (Artymowicz, Burrows, & Paresce 1989), and

applying equation (2), polarization "scans" $P(y, \Delta y)$ are obtained. Integrating these "scans" over all lines of sights (along the Y-axis) and again applying equation (2) yields the integral polarization P.

This algorithm, implemented in an original numerical code, is used to calculate the spatial distribution (scans) of polarization of a circumstellar dust disk with an arbitrary spatial density distribution, which could be measured from a distant point at an arbitrary viewing angle i.

3.2. *Geometry*

The global spatial dust distribution in the disk of β Pic, especially outside the innermost zone (>60–100 AU) is fairly well established (Artymowicz et al. 1989, 1990; Kalas & Jewitt 1995, 1996). Following these works, we represent the spatial number density distribution as

$$n(r, z) = n(r) \exp\left\{-\left[\frac{z/r_0}{\zeta(r)}\right]^{\gamma}\right\}, \quad \zeta(r) = \zeta_0\left(\frac{r}{r_0}\right)^{\eta}. \quad (3)$$

Here $n(r)$ specifies the radial dependence of the number density, and $r_0 = 6$. Following Artymowicz & Clampin (1997, hereafter AC97), we take in equation (3) a "smooth" bimodal radial distribution:

$$n(r) = [n_0(r/r_m)^{-1} + (r/r_m)^{\alpha}]^{-1}, \quad (4)$$

where $r_m = 60$ AU and n_0 and α are constants. The exponential term in equation (3) characterizes the vertical structure of the disk. Note that the coordinate z in equation (3) has a different meaning than before: it is measured from the symmetry plane of the disk. The parameter γ defines the vertical decrease. The vertical scale height ζ is a function of radius r (power law with index η).

The values of these parameters were estimated by Artymowicz et al. (1989) and by Kalas & Jewitt (1995), Kalas & Jewitt (1996). As the first step, in order to check how strongly the calculated polarization depends on the precise values of the parameters, we calculated the polarization for different values of them. It is known that the scattering and polarization functions derived empirically from zodiacal cloud measurements in the visual fit the observed polarization of β Pic quite well (Artymowicz 1997; Krivova et al. 1999). Thus for this part of the calculations we took these empirical functions (Weiß-Wrana 1983; Mann 1992). In Figure 2 we show polarization curves computed with different choices of the parameters that describe the disk geometry. For comparison, observational data in the R band for both wings are overplotted. As seen in Figure 2, variation of the parameters within the range given by the authors changes the resulting polarization much less than the observational errors. Moreover, the change concerns mostly the innermost zone for which observational data are not available. It should be noted that in accordance with Kalas & Jewitt (1995) the values of the parameters ζ_0 and i are interrelated: the larger i is, the smaller ζ_0 should be, so

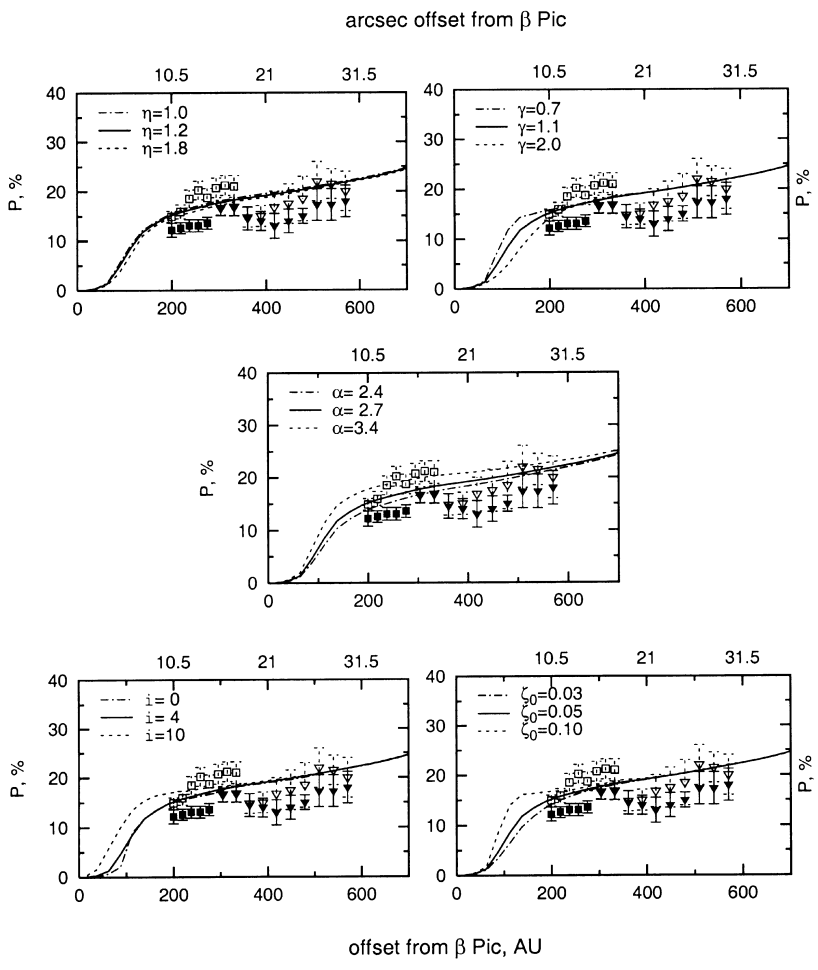

FIG. 2.—Polarization degree of β Pic for different parameters describing the disk geometry. Curves: modeling results. Symbols: observational data in the R band. *Triangles:* Gledhill et al. (1991). *Squares:* Wolstencroft et al. (1995). Data for the southwest wing are depicted as open symbols, whereas symbols showing the data in the northeast wing are filled. *Solid line:* a "standard" model, $\eta = 1.2$, $\gamma = 1.1$, $\alpha = 2.7$, $i = 4°$, $\zeta_0 = 0.05$.

that their influence is mutually compensated. For the index α, the range shown is even a bit broader than is the most probable one (between 2.6 and 3.1). In fact, even a more essential change of $n(r, z)$ does not influence the results strongly (Krivova et al. 1999).

Therefore, we take the values of the parameters either claimed in the papers cited as most probable or just in the middle of given ranges and fix them:

$$\eta = 1.2\,, \quad \gamma = 1.1\,, \quad \alpha = 2.7\,, \quad i = 4^\circ\,, \quad \zeta_0 = 0.05\,.$$

The corresponding polarization curve is shown as a solid line in each panel of Figure 2.

Less is known about the distribution of dust in the inner zone. Lagage & Pantin (1994) observed the inner part ($\lesssim$120 AU) of the disk with the resolution of 5 AU at 10 μm. Mouillet et al. (1997) detected the disk in scattered light down to 1.″5 from the star (29 AU). As was expected earlier (Artymowicz et al. 1990; Golimowski, Durrance, & Clampin 1993; Kalas & Jewitt 1995), the disk is getting thinner and the radial density profile becomes flatter than in the outer regions. In any case, the distribution of the dust within the innermost 60–100 AU does not influence the polarization outside 150–200 AU, so the precise shape of it (the first term in eq. [4]) is not important for our consideration. The disk extension is taken to be 1000 AU—close to the visible size of the disk in scattered light (e.g., Smith & Terrile 1987; Kalas & Jewitt 1994, 1995). The exact value is also unimportant as far as scattered light is concerned.

3.3. *Dust Grain Model*

To model optical properties of dust grains, classical Mie theory is used throughout this work. Using this theory, Voshchinnikov & Krügel (1999) have calculated polarization diagrams for various kinds of spherical and core-mantle particles. The results are found to be similar for particles of different material composition and structure and to be determined fundamentally by the particle sizes. Small (size parameter $x < 1$) and large ($x \gg 1$) particles give a smooth angular dependence of the polarization with a pronounced maximum at 90° and $\sim$70°, respectively. The polarization of intermediate-sized particles is a rapidly oscillating function of the scattering angle with repeated changes of sign. Similar results were obtained by many authors for different kinds of dust grains, including spheroids, cylinders, bispheres, and very fluffy aggregates arbitrarily aligned in space (see Voshchinnikov & Krügel 1999 for a more detailed discussion and references). Furthermore, as was shown by Lumme, Rahola, & Hovenier (1997), Mie theory proved to be workable for complex particles, with some exceptions for forward and backward scattering, which are of no concern here, because we do not consider the polarization in the innermost parts of the disk. Importantly, the same typical shapes of the polarization diagrams in different size regimes are also well seen in experimental data (e.g., Sassen 1981 and Neeves & Reed 1992 for small motes; Zerull & Giese 1974, Zerull et al. 1980, and Schuerman et al. 1981 for particles of intermediate size; and Weiß-Wrana 1983 and Killinger 1987 for large grains). The qualitative similarity of polarization patterns in alternative approaches and models enables the general features of the size distribution in the disk of β Pic to be elucidated (in particular, with Mie theory), whereas quantitative differences make conclusions about dust composition and structure more uncertain. Using non-Mie methods does not help much in that, because they are not universal, require arduous computations, and do not always show a much better agreement with the experimental results. Additional remarks about the dust composition and structure are made in subsequent sections.

3.3.1. *Dust Composition*

The observed 10 μm silicate band is indicative of the presence of silicates in the disk. Therefore we assume the grain material to be silicate (Laor & Draine 1993). We also tested dirty ice, other silicates (Ossenkopf, Henning, & Mathis 1992; Jäger et al. 1994; Dorschner et al. 1995), pure as well as with admixture of graphite/carbon (Laor & Draine 1993; Zubko et al. 1996) and of vacuum. Optical properties of the composite and porous grains were calculated using the effective medium theory (EMT).

In fact, our main conclusions are scarcely affected by the choice of the material (or by the particle structure). Such a choice plays rather a corrective role when it comes to exact values of the sizes (see, e.g., Figs. 3–7 in Voshchinnikov & Krügel 1999), but the general shape of the size distribution stands. More discussion is given in § 4.2.

3.3.2. *Dust Sizes*

3.3.2.1. Power Law

First, we consider a power-law size distribution

$$n(a) = n_0\, a^{-q}\,, \tag{5}$$

with minimum and maximum sizes of grains $a_{\min}$ and $a_{\max}$, respectively. The presence of large grains ($\gtrsim$2–4 μm) in the disk of β Pic is rather unquestionable; they are required to explain different kinds of observations (Paresce & Burrows 1987; Artymowicz et al. 1990; Chini et al. 1991; Zuckerman & Becklin 1993). They are also necessary to reproduce the observed polarization. Without large particles one can explain the value (but not the profile and the wavelength dependence!) of the observed polarization if only quite small particles (less than 0.1 μm) are present in the shell, which is physically improbable and contradicts, e.g., the observed colors of the disk. Therefore we fix the maximum size $a_{\max}$ to be 100 μm. Yet larger grains could also be present but are not important in our case, because they do not change the polarization.

Large particles alone, however, do not explain all the observations either. Micron-sized and smaller grains provide a better fit to *IRAS* and ground-based observations at 10–20 μm (Backman et al. 1992). They are also required to reproduce the silicate emission feature (Telesco & Knacke 1991; Knacke et al. 1993; Aitken et al. 1993). So the minimum size $a_{\min}$ and the index q are free parameters of our model.

The power-law size distribution is, in fact, not well suited to the case of β Pic, and makes explanation of all the observations mentioned above problematic. Reducing the dust sizes to explain the *IRAS* fluxes and the silicate feature and keeping therewith the power-law distribution makes the contribution of small and medium-sized grains too high to fit well the far-IR and millimeter data, the gray extinction, and the scattered radiation, as well as the observed wavelength and radial profile of the polarization (see § 4.1).

3.3.2.2. Modified Power Law

Another, more natural, way to choose the size distribution is to consider physical processes in the disk which settle this distribution. The dust disk around β Pic is thought to

be a steady state system with a number of sources and sinks that dynamically equilibrate each other (e.g., Artymowicz 1997). Dust needs to be continuously replenished by macroscopic bodies (planetesimals, comets) and, at smaller sizes, by collisional gain. Losses are mostly due to grain-grain collisions (at larger sizes) and radiation pressure removal (at smaller sizes). Furthermore, the disk is not isolated from the interstellar medium (ISM), and collisions between interstellar and disk grains cause simultaneous destruction of larger disk particles and additional production of fine debris; the possible influence of the ISM will be considered later.

At any moment, the β Pic disk contains two populations: (i) larger, long-lived grains in bound orbits, the lifetimes of which are limited by grain-grain collisions ($t_{\rm coll}$ of the order of thousands of years; see Artymowicz 1997), and (ii) smaller, short-lived grains blown away by radiation pressure in hyperbolic orbits, the lifetimes of which are just the times they need to cross the disk ($t_{\rm rad}$ of the order of hundreds of years). Using the solar system terminology (Zook & Berg 1975), we will refer to the two populations as α- and β-meteoroids, respectively. These populations are separated roughly by a certain grain radius, a_0, such that the radiation pressure to stellar gravity ratio $\beta(a_0) = \frac{1}{2}$ (Burns, Lamy, & Soter 1979). Grains with $a \gtrsim a_0$ are predominantly α-meteoroids, while those with $a \lesssim a_0$ are β-meteoroids. The particular value of a_0 depends on a grain model, but for all plausible materials lies in the range 1–5 μm. In the numerical examples that follow we use the modeled "asteroidal dust" of Wilck & Mann (1996) for which $a_0 = 2.2$ μm (as for silicate of Laor & Draine 1993).

Consider α-meteoroids first ($a > a_0$). Following AC97, we use the radial profile of number density given by equation (4) and assume that (i) the number density of grains is uniform vertically within the disk with the opening angle $\epsilon = 14°$, and (ii) the large grains in the disk are supplied by sources in the disk with the size distribution $n(a) \propto a^{-q}$, $q \approx 3.5$, which is a good approximation for particles produced by collisional fragmentation (see, e.g., Dohnanyi 1969) and activity of comets (e.g., Fulle et al. 1995). Under these assumptions, equation (4) takes the expanded form, giving the number density of grains with radii $a_1 \le a \le a_2$ ($a_0 \le a_1$) at the distance r from the star:

$$n_\alpha(r; a_1, a_2) \approx \frac{2\tau_m}{\pi\epsilon a_0^2 r_m}\left[\left(\frac{r}{r_m}\right)^{-1} + \left(\frac{r}{r_m}\right)^{2.7}\right]^{-1} \times \frac{q-3}{q-1}\left[\left(\frac{a_1}{a_0}\right)^{1-q} - \left(\frac{a_2}{a_0}\right)^{1-q}\right], \quad (6)$$

where $\tau_m \equiv \tau(r_m) = 7.6 \times 10^{-3}$ is the maximum normal optical depth (AC97).

Now we consider β-meteoroids ($a < a_0$). They have $\beta > \frac{1}{2}$ and will be swept out by the stellar radiation pressure. AC97 used an elaborate collisional model to calculate the mass-loss rate per unit distance interval, $\dot{M}(r)$, due to (i) mutual collisions of disk grains and (ii) collisions of disk grains with ISM particles. Now we focus on the first of these, i.e., internal collisions, and return to the second in § 5.1. As small grains are continuously produced at the rate $\dot{M}(r)$, and are simultaneously blown away by radiation pressure, steady state number densities of these grains should be settled in the system. First, neglecting the initial velocity of a small grain due to the momentum transfer from the projectile, but taking into account the initial circular Keplerian velocity due to the disk rotation, the velocity that a particle ejected at a distance r_0 will develop at a distance r is

$$v(r_0, r; a) = \sqrt{GM\left[\frac{2(1-\beta)}{r} + \frac{(2\beta-1)}{r_0}\right]} \quad \left(\beta \ge \frac{1}{2}\right), \quad (7)$$

which depends on the size a through $\beta = \beta(a)$. Second, we assume that the *initial* size distribution of collisional debris is again a power law $n(a) \propto a^{-q}$ with $q \approx 3.5$. Straightforward calculations lead to the number density of grains with radii $a_1 \le a \le a_2$ ($a_2 \le a_0$) at the distance r from the star:

$$n_\beta(r; a_1, a_2) = \frac{1}{2\pi \sin\epsilon}\frac{1}{r^2}\int_0^r \frac{\dot{M}(r_0)/m_0}{v(r_0, r; a_1, a_2)}\, dr_0 \times \frac{4-q}{q-1}\left[\left(\frac{a_1}{a_0}\right)^{1-q} - \left(\frac{a_2}{a_0}\right)^{1-q}\right]. \quad (8)$$

Here $v(r_0, r; a_1, a_2)$ is given by equation (7) after the substitution $\beta = \bar{\beta}(a_1, a_2)$ (the mean β ratio of the grains with radii $a_1 \le a \le a_2$); m_0 is the mass of an a_0 grain.

The number densities computed numerically from equations (6) and (8) are shown in Figure 3. In each panel, the bold solid line depicts the distribution of the main population ($a \ge a_0$ grains). Medium-thickness lines show the dis-

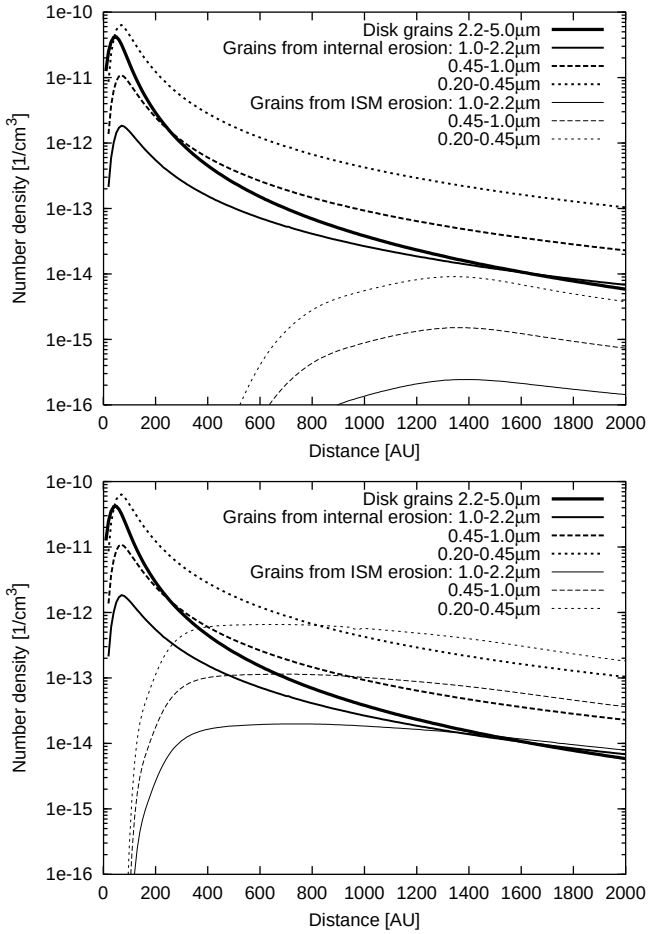

FIG. 3.—Calculated number density profiles of several populations of grains in the β Pic disk: α-meteoroids (*bold solid line*), β-meteoroids produced by mutual grain-grain collisions (*medium-thickness lines*), β-meteoroids produced by disk grain collisions with interstellar particles (*thin lines*) in two ISM models: ISM model 1 (*top*) and ISM model 5 (*bottom*) of AC97.

tributions of smaller grains (in three size ranges equally spaced in log scale) produced by internal collisions. These results show that the disk should contain quite a large amount of submicron dust due to internal collisions.

Consider now the size distribution of grains expected from our calculations. Recall that the disk grains were assumed to have initially a standard power-law size distribution with the exponent $q = 3.5$. However, small grains become β-meteoroids and move within the disk in unbound trajectories with size-dependent (β-dependent) velocities. This modifies the size distribution of small grains. The size distribution calculated with our model is shown in Figure 4. The distribution has a steplike drop at $a = a_0 = 2.2$ μm and is bent at smaller sizes around the maximum of $\beta(a)$, at $0.1 \lesssim a \leq 2.2$ μm. Obviously, the sharpness of the step at $a = a_0$ is just an artifact of the modeling (a direct consequence of the assumption that *all* grains with $\beta > \frac{1}{2}$ get in unbound orbits and *all* with $\beta > \frac{1}{2}$ stay in bound trajectories, which would be true only if the parent grains/source bodies had initially circular Keplerian velocities). In reality, the curve is smooth, but the very *existence* of a drop near a_0 must be real. The strength of the drop is, generally, distance dependent: in our model, it is larger closer to the star. Note that a similar feature of the size distribution—a depletion of submicron-sized dust with respect to large particles—has long been known for the zodiacal cloud in the solar system (Grün et al. 1985). Even sharper "steps," like the one in Figure 4, are predicted in the collisional modeling of the dust cloud in the inner solar system (Ishimoto & Mann 1999).

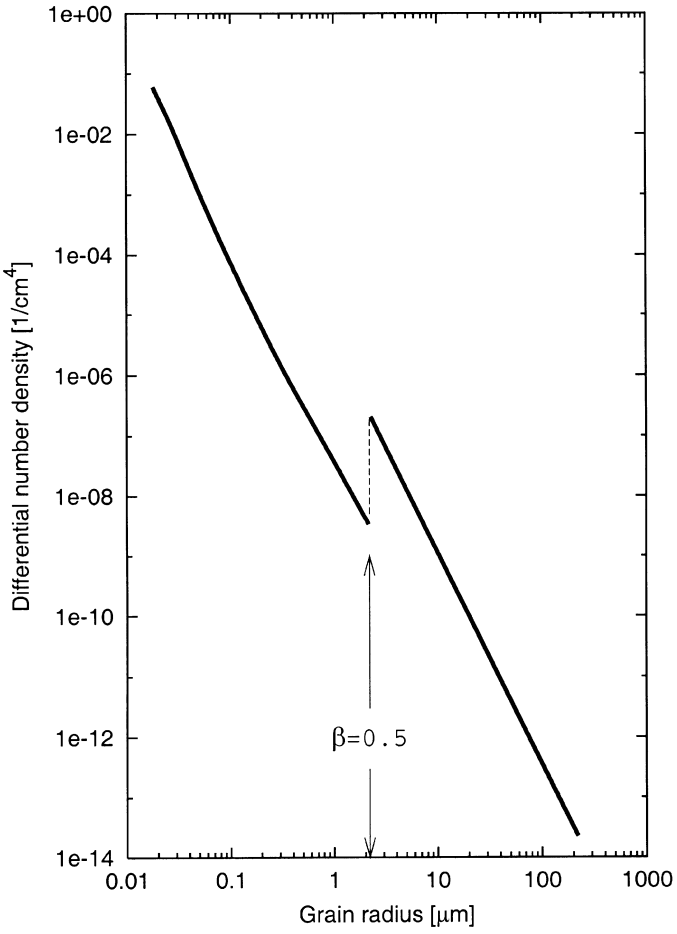

FIG. 4.—Calculated size distribution of grains in the β Pic disk at $r = 100$ AU.

4. MODELING OF POLARIZATION. RESULTS

4.1. *Power-Law Size Distribution*

Power-law size distributions for the dust were assumed for studies of the β Pic polarization by Scarrott et al. (1992) and by Voshchinnikov & Krügel (1999). Scarrott et al. (1992) showed that the R-band polarization could be explained with silicate grains having sizes between 0.01 and 3 μm and a size index $q = 4.0 \pm 0.3$. Their model, however, does not reproduce the wavelength dependence of the polarization (these observations were not yet available), and the predicted colors of the disk are redder than the observed ones. Voshchinnikov & Krügel (1999) found that the observed values of the polarization could be explained if only large particles ($\gtrsim$1–5 μm depending on the refractive index) are present. They noticed, however, that these mixtures give too red colors and do not fit the wavelength dependence. This agrees with our results. Then to make the colors bluer one should *include the smaller grains* into the model. However, extrapolating the traditional power-law size distribution down to small sizes poses other difficulties. First, the submicron particles produce polarization smaller than the observed one. Second, the interaction of stellar radiation with the submicron and smaller particles is quite different in the B and I bands, producing wavelength dependence of the polarization different from the observed dependence (decreasing with the wavelength).

One can reduce the difficulty by decreasing the index q in the power law with respect to $q \approx 3.5$ or, in other words, by *lowering the fraction of the smaller grains*. As an example, we show in Figure 5 the results for the disk consisting of silicate grains (Laor & Draine 1993) with sizes between 0.005 and 100 μm and with the index $q = 2.7$. It is seen that the model explains reasonably well the observed polarization in the northeast wing. The predicted colors are also in good agreement with the observations. The relative colors, Q_B, Q_V, and Q_R, are 0.88,0.92, and 0.97, respectively. Contrary to the conclusion of Voshchinnikov & Krügel (1999), similar results could also be obtained for grains with a different composition; only the index q should be a little bit modified (for a smaller refractive index it should be a bit reduced, so that the contribution of the larger grains is correspondingly larger; cf. Figs. 6 and 7 in Voshchinnikov & Krügel 1999).

Two remarks need to be made here. First, independent of the refractive index, we could not find such a model which would also fit the data for the southwest wing. The polarization in it is larger, which means that more large grains should be included to explain it (even smaller q). With the standard power law this implies that the contribution of medium-sized ($\sim$0.1–2 μm) grains will also increase. However, these grains, the sizes of which are comparable to the wavelength, produce quite a different polarization in the B and R bands, with the polarization in B being much higher than that in R, which contravenes observations.

Second, if the component of small grains (smaller than a few microns) consists of materials with very small refractive indices, such as water ice (unless it is highly dirty, e.g., the sample with the volume fraction of the magnetite inclusions $f = 0.1$ in the paper of Mukai 1989), the modeled polarization is always below the observed values. The same is true for highly porous particles (the filling factor of the material

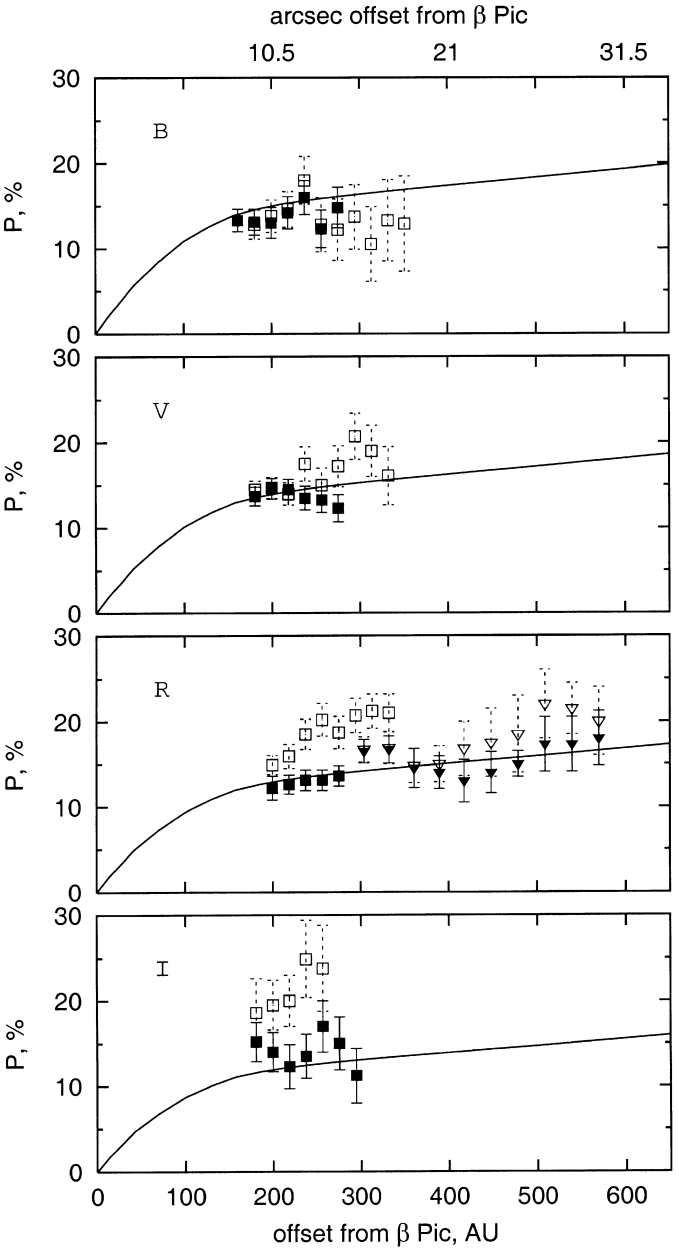

FIG. 5.—Modeled polarization degree of the disk of β Pic in B, V, R, I (*solid lines*). The disk is assumed to consist of silicate grains with $a_{\min} = 0.005$ μm, $a_{\max} = 100$ μm, $q = 2.7$. Symbols for observational data are as in Fig. 2.

is $f \lesssim 50\%$). Therefore, the component of the "small" particles is unlikely either to consist of pure water ice or to be very porous.

Note that the latter conclusion about the porosities should be taken with caution. To consider very porous aggregates like those suggested by Li & Greenberg (1998), a special approach (see, e.g., Nakamura 1998) may be more relevant. However, EMT is still expected to give qualitatively correct results. For example, a very low degree of polarization for porous grains was found with the EMT in study of the polarization of Herbig Ae/Be stars (Il'in & Krivova 2000; Krivova & Il'in 2000) and later confirmed using more accurate discrete dipole approximation (DDA) calculations of the dust optical properties (Krivova, Kimura, & Il'in 2000, in preparation). In these DDA calculations, an increase of the subgrain sizes caused an increase of the polarization, which was, however, not large enough to explain the observed polarization.

4.2. *Modified Size Distribution*

Discussion in § 4.1 made it clear that the whole set of observations of the polarization and colors of β Pic can be explained only if both large (larger than a few microns) and small particles are present in the disk. The amount of small grains, especially submicron, up to micron-sized grains should, however, be less than would be expected from the power-law distribution with index $q \approx 3.5$. Interestingly, a similar modification—a decrease of the power-law index down to 3.0—was found by Pantin, Lagage, & Artymowicz (1997) to be the best fit of mid-IR images and *IRAS* fluxes.

Now we apply the size (and radial) distributions obtained from the consideration of the dynamics of the grains (see § 3.3.2). We implement a two-component dust model. One component is α-meteoroids—large (>3 μm) grains, the distribution of which is given by equation (6). Another component is β-meteoroids—the particles smaller than 3 μm, produced by collisions of larger grains, but moving in unbound orbits out from the star; the distribution of β-meteoroids is given by equation (8). The radial distribution of them is slightly modified (see Fig. 3) in comparison to the large grains, so that the power-law index α in equation (4) is about 2.5, whereas for large grains 2.7 is taken. This difference in the radial slope is, however, not important (see § 3.2 and Fig. 2). It is more important that the amount of smaller grains is lower by 1 or 2 orders of magnitude than it would be if the radiation pressure did not blow them away from the star (see Fig. 4).

A direct application of the dust size and radial distributions (eqs. [6] and [8]) immediately provides a good fit to the observational data in the southwest wing; see the right-hand panels in Figure 6. The relative colors of the model Q_B, Q_V, and Q_R are 0.91 , 0.92, and 0.95, respectively, i.e., close to the observed values (see § 2.2). The albedo of the dust is 0.6, which is also in good agreement with the values predicted from modeling of other data (Artymowicz et al. 1989, 1990; Backman et al. 1992; see also discussions in Artymowicz 1994,1997). Since in our model the main contribution into the total cross section area is made by large grains, but small grains are present as well, we expect that the model is also consistent with the other observational data discussed in § 1. Interestingly, the calculated scattered brightness in the K band is about 50%–70% higher than in the R band; the observed brightnesses differ roughly by a factor of 2 (Mouillet et al. 1997). The predicted polarization in the K band is still larger but only slightly (by less than 0.5%) than in the I band. We have also made calculations for the U band. The polarization is lower by 1%–2% than in the B band, thus decreasing further with the wavelength. The color does not change ($Q_U = 0.93$ for this particular model).

As the difference in the radial distribution of two components is small, it is possible to replace the model given by equations (6)–(8) with a simpler one, which is more convenient for computations. One can take a standard power-law size distribution with the exponent $q = 3.5$ and minimum and maximum sizes $a_{\min}$, $a_{\max}$ of 0.005 μm and 100 μm, respectively, but with a drop (of a factor of ~ 20 in this particular model) in the number densities at about 2–3 μm (for the silicate), where the parameter β is equal to $\frac{1}{2}$ (cf. Fig. 4). The precise position (within the range ~ 1–10 μm) and

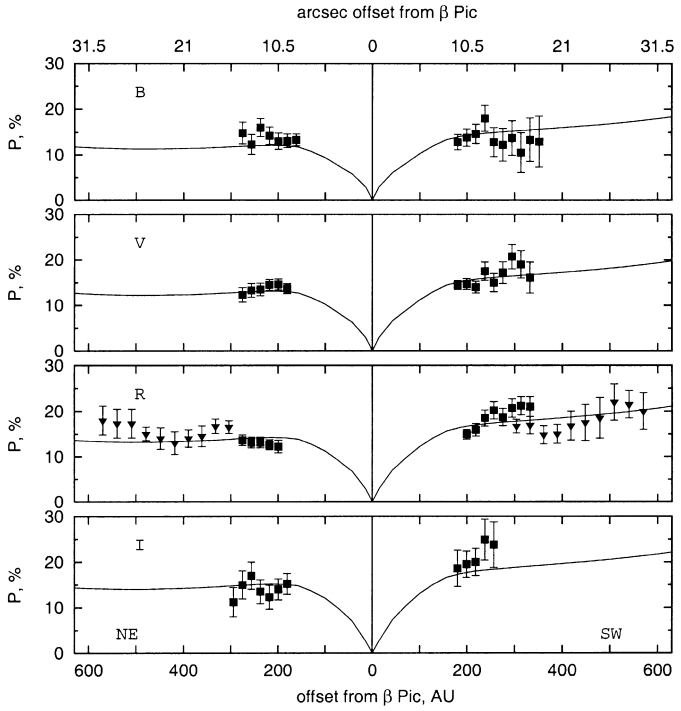

FIG. 6.—Polarization degree of the disk of β Pic with the dynamically justified size distribution. For the southwest wing (*right*) a two-component dust model is used: α-meteoroids with sizes $a > 3$ μm, $q = 3.5$, $\alpha = 2.7$ and β-meteoroids with $a < 3$ μm, $q = 3.5$, $\alpha = 2.5$. See § 3.3.2 for details. For the northeast wing (*left*) a three-component dust model is implemented with the same two components as for the southwest wing and an additional component of small grains (< 3 μm) produced by collisions with ISM particles. See § 5.1 for details.

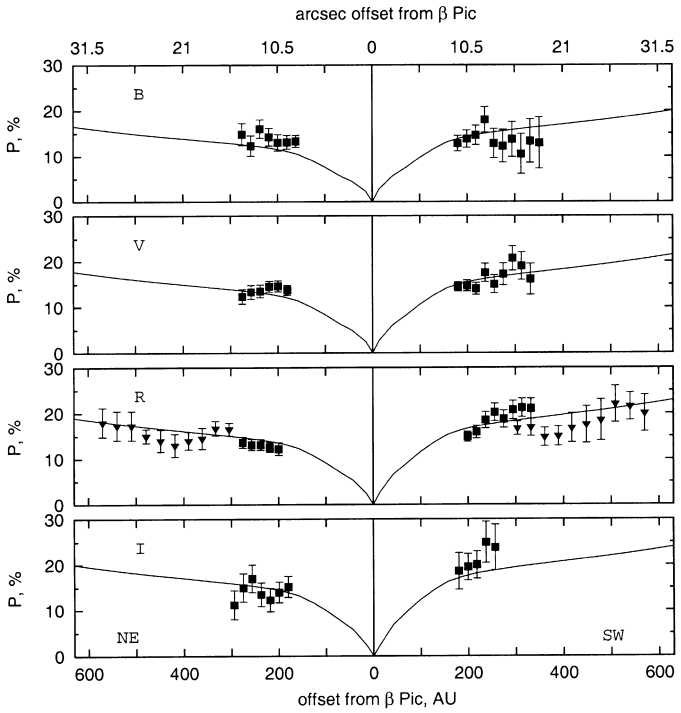

FIG. 7.—Polarization degree of the disk of β Pic with the power-law size distribution and depletion of small grains. In contrast to Fig. 6, a simplified one-component dust model is implemented. The radial distribution ($\alpha = 2.7$) is the same for all grains including those produced in collisions with ISM particles. The size distribution is a power law with a drop at 3 μm like that shown in Fig. 4. The drop is larger (about 20) in the southwest wing (*right*) and smaller (about 15) in the northeast wing (*left*).

the strength ($\sim$10–100) of the drop depend on the material used, as β does. The polarization obtained for this model is shown in Figure 7 in the right-hand panels for the southwest wing. The relative colors of the model and the albedo are also close to those in the two-component dust model shown in Figure 6: $Q_B = 0.93$, $Q_V = 0.93$, and $Q_R = 0.96$, $\Lambda \approx 0.6$.

It should be mentioned here that, again, for significantly porous grains and very transparent materials the agreement with the observations is generally worse. The best fit to the polarimetric observations is obtained for the positions of the drop shifted by some 5–10 μm to the larger sizes in comparison to a_0, whereas for silicate grains, as in Laor & Draine (1993) and Ossenkopf et al. (1992), olivines or pyroxenes with a moderate fraction of iron [Fe/(Mg + Fe) $\approx$ 0.4–0.6] from Dorschner et al. (1995), both the position of the drop and the parameter a_0 coincide within 1–2 μm, sufficiently well within the uncertainties of the model.

5. ASYMMETRY OF THE WINGS

The observed disk of β Pic is known to possess a number of asymmetries and warps (e.g., Kalas & Jewitt 1995). These comprise a general brightness/radial extension asymmetry of two wings, their width asymmetry, and warplike disk asymmetries, some of which are especially pronounced in inner parts of the disk. Here we consider only the first of them, a global brightness/extension asymmetry, reflected in the difference in the observed polarization in the northeast and southwest wings of the disk.

To fit the northeast wing observations, one should increase slightly a contribution of the smaller grains. The results obtained by reducing the drop in the size distribution by about 25% are shown in Figure 7 in the panels for the northeast wing. The relative colors are 0.98–1.0 for all bands.

5.1. *Disk-ISM Interaction as a Possible Source of Asymmetry*

What could lead to such a difference between dust properties of the wings? While more local disk asymmetries, such as inner disk warps, are usually credited to the presence of a planetary perturber at a small distance, attributing the brightness/polarization asymmetry considered here to an influence of a presumed planet faces difficulties (Wolstencroft et al. 1995; Artymowicz 1997). Indeed, it is not clear at present through which mechanism a presumed planet could affect outer parts of the disk, producing a general brightness/size asymmetry of the two wings. Here we consider another conceivable mechanism—interactions of the dust disk with the ISM (Artymowicz 1997). The interstellar grains, because they are small, experience the radiation pressure repulsion but are able to penetrate the upstream side of the disk, reaching distances of several hundreds of AU from the star. Thus the ISM flow erodes the upstream part of the circumstellar disk (Lissauer & Griffith 1989). This "sandblasting" is not only destructive: it also produces, via catastrophic and cratering collisions, fine debris in this part of the disk (Whitmire, Matese, & Whitman 1992). Note that the dust production in the Kuiper Belt region of the solar system was suggested to stem partly from the ISM erosion (Yamamoto & Mukai 1998). The number densities of the fine dust grains produced by the ISM erosion can be calculated with equation (8), used before to investigate internal erosion in the disk. What

one should do is only to replace the "source function" $\dot{M}(r)$ describing internal collisions with another one, obtained by AC97 for ISM collisions.

The computed densities of different-sized grains produced by collisions of ISM particles are shown in Figure 3 with thin lines. Two panels in Figure 3 correspond to two models of the ISM adopted in AC97. The top panel is for "ISM model 1," which AC97 believe to be the most plausible. The ISM spatial density is assumed to be 4.4×10^{-25} g cm^{-3}, the relative ISM-star velocity $v_\infty = 8.6$ km s^{-1}, and the ISM flux streams at 45° to the disk plane. The bottom panel is for an incoming ISM flux that is twice as fast (AC97's model 5), i.e., $v_\infty = 17.2$ km s^{-1}, and the angle is 15°. Note that the results do not depend much on this angle. The erosion profiles are similar even for quite different streaming angles of 15° and 75° (cf. the top and bottom panels in AC97's Fig. 6). Thus a close accidental alignment of the ISM velocity vector with a certain direction is not required for the mechanism to work out.

These results show that the amount of submicron- and even micron-sized dust, produced by the ISM impacts in the upstream wing of the disk, is not negligibly small—at least in more "aggressive" ISM models like "ISM model 5" of AC97. For the latter model, e.g., the densities of 1 to 2 μm grains produced by ISM impacts are comparable, in outer parts of the disk, to those formed by internal collisions, and also to the number densities of the "stable" disk grains.

There are some reasons to think that the effect of ISM erosion *may* be at least as significant as in AC97's "extreme" ISM model 5. Indeed, the effect depends strongly on (i) the spatial density and size distribution of the ISM grains; (ii) the relative velocity ISM-star. As far as the first factor is concerned, AC97 seem to underestimate the effect of very large (up to $\sim$3–30 μm) ISM grains, evidenced by excess interstellar emission at millimeter wavelengths (Rowan-Robinson 1992; Kim & Martin 1996), by interpretation of *Pioneer 10* and *11* dust impact data in the outer solar system (Humes 1980) as being due to $\sim$10 μm interstellar dust impacts (Grün et al. 1994), and, more directly, by radar observations of interstellar meteors on Earth (Taylor, Baggaley, & Steel 1996; Meisel, Janches, & Mathews 1999). In AC97's ISM model 8, the interstellar grains are assumed to have $a = 1$ μm and spatial density of 1.6×10^{-27} g cm^{-3}. Assuming higher densities such as 2.8×10^{-26} g cm^{-3} reported by Mann & Kimura (1999), one gets the amounts of collisional debris close to those predicted by AC97's ISM model 5. As regards factor (ii), AC97 consider the motion of β Pic relative to the local standard of rest (LSR) ($v_* = 5$ km s^{-1} and estimate the (actually unknown) velocity of the ISM itself relative to the LSR $v_{\rm ISM} = 7$ km s^{-1} to derive the value $v_\infty = (v_*^2 + v_{\rm ISM}^2)^{1/2} = 8.6$ km s^{-1}. The latter value is likely to be only *statistically* correct. However, for a particular star, β Pic in our case, the actual value v_∞ may be as high as 12 km s^{-1}, if the direction of $\boldsymbol{v}_{\rm ISM}$ is favorable.

For these reasons, in calculations that follow we use the number densities of ISM-generated debris of AC97's ISM model 5 (Fig. 3, *bottom panel*).

5.2. *Polarization in the Northeast Wing*

To describe the collisional debris produced by interstellar grain impacts, we add the third component to the model applied in § 4.2. The size distribution of the third component is the same as that of the second component (grains produced by the internal collisions). Therefore, inclusion of the third component is, to a first approximation, equivalent to reduction of the drop in the number densities between large and small grains, which justifies the model shown in the left panel of Figure 7.

However, the third component has quite a different radial distribution; it is actually absent in the inner zone (about 300 AU), and farther out the number density of these grains slopes only slightly outward, so that in the outer regions there are even more such particles than the particles produced in the mutual collisions of the disk grains. Taking into account the radial dependence of the third component, we get the result shown in the left panels of Figure 6. The albedo is only 2%–4% higher than in the model for the southwest wing and, as distinct from the northeast wing, grows by a few percent with the offset distance. The colors are 0.93–0.96, are similar in the two wings, and are almost constant with the offset. The maximum increase from 100 to 1000 AU is less than 4% in the B band. Closer to the star the colors drop by 30%–40% in B and by less than 20%–30% in the other bands. The inner drop, however, depends slightly on the precise geometry of the disk in this region (see § 2).

Noteworthy also is the difference in the brightnesses of the wings. The northeast wing in our model is slightly brighter (by about 20% at 400 AU) than the southwest wing, as was really observed (e.g., Kalas & Jewitt 1995). Having an additional component of the small dust, a contribution of which is growing outward, the northeast wing should be visible slightly farther from the star, which is actually observed (Smith & Terrile 1987; Kalas & Jewitt 1995). Also in agreement with observations (Golimowski et al. 1993; Kalas & Jewitt 1995), the radial density and brightness distributions for this dust component, and thus for the northeast wing, are flatter in our model.

6. CONCLUSIONS

In this paper we model the polarization of the β Pic disk as a function of wavelength and offset distance from the star. What is more, we fit the data in each of the two wings separately. The geometry of the disk is described following the results obtained from the study of the images in scattered light (Artymowicz et al. 1989; Kalas & Jewitt 1995). However, we show that the precise values of the geometrical parameters have no influence on the results for the region where the observations are available; the uncertainties of the models would only weakly affect the resulting polarization in the inner parts of the disk. In contrast, the size distribution of dust plays a crucial role and therefore can be tightly constrained from the observations. Changes in the refractive index (i.e., in the material composition and/or porosity) of the grains affect the results as well, but much more weakly than the size distribution does.

Our conclusions are as follows:

1. The observed polarization and colors of the disk of β Pic could be best explained if the particles in a wide range of sizes are present in the disk, but the amount of small grains is smaller than would be expected from extrapolation of a commonly used power-law distribution with the exponent $q = 3.5$ down to smaller sizes. The number densities of these grains (smaller than 2–3 μm in the case of silicate and slightly more for other compositions) is about a factor of 10–100 smaller than would be expected from the power-law distribution. With this size distribution, the small particles are

still of importance for the polarization and colors. Not only is this size distribution found as a best fit to the polarimetric and colorimetric observations; it is also justified dynamically. The depletion of small grains is caused by stellar radiation pressure that sweeps them out of the star, leading to tenfold or hundred-fold shorter lifetimes in the disk.

2. Although conclusion 1 remains valid regardless of the dust composition and structure, better agreement with observations is obtained for compact (or just slightly porous) silicate particles. The component of small grains is unlikely to be highly porous, though a verification of this result in a more accurate approach is desirable.

3. The observed asymmetry in the polarization of two wings can be explained in terms of slightly different size distributions. More small grains are present on the northeast side of the disk (by 20%–30%).

4. One possibility is that such an asymmetry in the size distributions in two wings could result from the influence of the interstellar medium. Interstellar grains penetrating into the disk and colliding with the circumstellar grains could produce the required amount of additional small grains. Not ruling out other conceivable scenarios, we have demonstrated that under appropriate conditions the ISM bombardment would account for the observed polarization asymmetry.

We thank V. B. Il'in, H. Kimura, and N. N. Kiselev for discussions and the referee for a thorough review of the manuscript. Part of this work was supported by the Bundesministerium für Bildung, Wissenschaft, Forschung und Technologie (BMBF). A. K. is an Alexander von Humboldt Fellow at the Max-Planck-Institut für Aeronomie.

REFERENCES

Aitken, D., Moore, T., Roche, P., Smith, C., & Wright, C. 1993, MNRAS, 265, L41
Artymowicz, P. 1988, ApJ, 335, L79
———. 1994, in Circumstellar Dust Disks and Planet Formation, ed. R. Ferlet & A. Vidal-Madjar (Gif-sur-Yvette: Editions Frontières), 47
———. 1997, Annu. Rev. Earth Planet. Sci., 25, 175
Artymowicz, P., Burrows, C., & Paresce, F. 1989, ApJ, 337, 494
Artymowicz, P., & Clampin, M. 1997, ApJ, 490, 863 (AC97)
Artymowicz, P., Paresce, F., & Burrows, C. 1990, Adv. Space Res., 10, 81
Aumann, H. H. 1988, AJ, 96, 1415
Aumann, H. H., et al. 1984, ApJ, 278, L23
Aumann, H. H., & Probst, R. G. 1991, ApJ, 368, 264
Backman, D. E., & Gillett, F. C. 1987, in Cool Stars, Stellar Systems, and the Sun, ed. J. L. Linsky & R. E. Stencel (Lecture Notes in Physics 291; Berlin: Springer), 340
Backman, D. E., & Paresce, F. 1993, in Protostars and Planets III, ed. E. H. Levy, J. I. Lunine, & M. S. Matthews (Tucson: Univ. Arizona Press), 1253
Backman, D. E., Witteborn, F. C., & Gillett, F. C. 1992, ApJ, 385, 670
Burns, J. A., Lamy, P. L., & Soter, S. 1979, Icarus, 40, 1
Cheng, K. P., Bruhweiler, F. C., Kondo, Y., & Grady, C. A. 1992, ApJ, 396, L83
Chini, R., Krügel, E., Kreysa, E., Shustov, B., & Tutukov, A. 1991, A&A, 252, 220
Crifo, F., Vidal-Madjar, A., Lallement, R., Ferlet, R., & Gerbaldi, M. 1997, A&A, 320, L29
Dohnanyi, J. S. 1969, J. Geophys. Res., 74, 2531
Dorschner, J., Begemann, B., Henning, T., Jäger, C., & Mutschke, H. 1995, A&A, 300, 503
Fajardo-Acosta, S. B., Telesco, C. M., & Knacke, R. F. 1998, AJ, 115, 2101
Fulle, M., Colangeli, L., Mennella, V., Rotundi, A., & Bussoletti, E. 1995, A&A, 304, 622
Gledhill, T. M., Scarrott, S. M., & Wolstencroft, R. D. 1991, MNRAS, 252, 50P
Golimowski, D. A., Durrance, S. T., & Clampin, M. 1993, ApJ, 411, L41
Grün, E., Zook, H. A., Fechtig, H., & Giese, R. H. 1985, Icarus, 62, 244
Grün, E., Gustafson, B., Mann, I., Baguhl, M., Morfill, G. E., Staubach, P., Taylor, A., & Zook, H. A. 1994, A&A, 286, 915
Hünsch, M., Schmitt, J. H. M. M., Sterzik, M. F., & Voges, W. 1999, A&AS, 135, 319
Hünsch, M., Schmitt, J. H. M. M., & Voges, W. 1998, A&AS, 132, 155
Humes, D. H. 1980, J. Geophys. Res., 85, 5841
Il'in, V. B. & Krivova, N. A. 2000, Astron. Lett., 26, 379
Ishimoto, H., & Mann, I. 1999, Planet. Space Sci., 47, 225
Jäger, C., Mutschke, H., Begemann, B., Dorschner, J., & Henning, T. 1994, A&A, 292, 641
Kalas, P., & Jewitt, D. 1994, in Circumstellar Dust Disks and Planet Formation, ed. R. Ferlet & A. Vidal-Madjar (Gif-sur-Yvette: Editions Frontières), 371
———. 1995, AJ, 110, 794
———. 1996, AJ, 111, 1347
Killinger, R. T. 1987, Ph.D. thesis, Ruhr-Univ. Bochum
Kim, S.-H., & Martin, P. G. 1996, ApJ, 462, 296
Knacke, R. F., Fajardo-Acosta, S. B., Telesco, C. M., Hackwell, J. A., Lynch, D. K., & Russell, R. W. 1993, ApJ, 418, 440
Korhonen, T., & Reiz, A. 1986, A&AS, 64, 487
Krautter, J. 1980, A&AS, 39, 167
Krivova, N. A., & Il'in, V. B. 2000, Icarus, 143, 159
Krivova, N. A., Mann, I., & Krivov, A. V. 1999, in Meteoroids 1998, ed. W. J. Baggaley & V. Porubčan (Bratislava: Astron. Inst. Slovak Acad. Sci), 291
Lagage, P., & Pantin, E. 1994, Nature, 369, 628
Laor, A., & Draine, B. T. 1993, ApJ, 402, 441
Lecavelier des Etangs, A., et al. 1993, A&A, 274, 877
Leroy, J. L. 1993, A&AS, 101, 551
———. 1999, A&A, 346, 955
Leroy, J. L., & Le Borgne, J. F. 1989, A&A, 223, 336
Li, A., & Greenberg, J. M. 1998, A&A, 331, 291
Lissauer, J. J., & Griffith, C. A. 1989, ApJ, 340, 468
Lumme, K., Rahola, J., & Hovenier, J. W. 1997, Icarus, 126, 455
Mann, I. 1992, A&A, 261, 329
Mann, I., & Kimura, H. 1999, J. Geophys. Res., 105, 10317
Mannings, V., & Barlow, M. J. 1998, ApJ, 497, 330
Martin, P. G. 1978, Cosmic Dust: Its Impact on Astronomy (Oxford: Clarendon)
Mathewson, D. S., & Ford, V. L. 1970, MmRAS, 74, 139
Meisel, D. D., Janches, D., & Mathews, J. D. 1999, paper presented at ACM-99 Conf. 20.05 (Cornell Univ.)
Mouillet, D., Lagrange, A.-M., Beuzit, J.-L., & Renaud, N. 1997, A&A, 324, 1083
Mukai, T. 1989, in Evolution of Interstellar Dust and Related Topics, ed. A. Bonetti, J. M. Greenberg, & S. Aiello (Amsterdam: North-Holland), 397
Nakamura, R. 1998, Earth Planets Space, 50, 587
Neeves, A. E., & Reed, W. A. 1992, Appl. Opt., 31, 2072
Ossenkopf, V., Henning, T., & Mathis, J. S. 1992, A&A, 261, 567
Pantin, E., Lagage, P. O., & Artymowicz, P. 1997, A&A, 327, 1123
Paresce, F., & Burrows, C. 1987, ApJ, 319, L23
Rowan-Robinson, M. 1992, MNRAS, 258, 787
Sassen, K. 1981, Appl. Opt., 20, 185
Scarrott, S. M., Draper, P. W., & Gledhill, T. M. 1992, in Dusty Discs, ed. P. M. Gondhalekar, 8
Schröder, K. P., Hünsch, M., & Schmitt, J. H. M. M. 1998, A&A, 335, 591
Schröder, R. 1976, A&AS, 23, 125
Schuerman, D. W., Wang, R. T., Gustafson, B. Å. S, & Schaefer, R. W. 1981, Appl. Opt., 20, 4039
Serkowski, K. 1968, ApJ, 154, 115
Smith, B. A., & Terrile, R. J. 1987, BAAS, 19, 829
Sobolev, V. V. 1985, Theoretical Astrophysics (Moscow: Nauka)
Taylor, A. D., Baggaley, W. J., & Steel, D. I. 1996, Nature, 380, 323
Telesco, C. M., & Knacke, R. F. 1991, ApJ, 372, L29
Telesco, C. M., Decher, R., Becklin, E. E., & Wolstencroft, R. D. 1988, Nature, 335, 51
Tinbergen, J. 1982, A&A, 105, 53
Turon, C., et al. 1993, Bull. Inf. CDS, 43, 5
Voshchinnikov, N. V., & Krügel, E. 1999, A&A, 352, 508
Weiß-Wrana, K. 1983, A&A, 126, 240
Whitmire, D. P., Matese, J. J., & Whitman, P. G. 1992, ApJ, 388, 190
Wilck, M., & Mann, I. 1996, Planet. Space Sci., 44, 493
Wolstencroft, R. D., Scarrott, S. M., & Gledhill, T. M. 1995, Ap&SS, 224, 395
Yamamoto, S., & Mukai, T. 1998, A&A, 329, 785
Zerull, R. H., & Giese, R. H. 1974, in Planets, Stars and Nebulae Studied with Photopolarimetry, ed. T. Gehrels (Tucson: Univ. Arizona Press), 901
Zerull, R. H., Giese, R. H., Schwill, S., & Weiß, K. 1980, in Light Scattering by Irregularly Shaped Particles, ed. D. W. Schuerman (New York: Plenum), 273
Zook, H. A., & Berg, O. E. 1975, Planet. Space Sci., 23, 183
Zubko, V. G., Mennella, V., Colangeli, L., & Bussoletti, E. 1996, MNRAS, 282, 1321
Zuckerman, B., & Becklin, E. E. 1993, ApJ, 414, 793